Supplementary Materials

Table S1 CMIP6 global climate models employed for ensemble storm surge projections

CMIP6 model	Resolution (lon x lat)
MPI-ESM1-2-HR	0.9375° x 0.9375°
CNRM-CM6-1-HR	0.5 x 0.5
EC-Earth3	0.7 x 0.7
HadGEM3-GC31-MM	0.833 x 0.556
BCC-CSM2-MR	1.125° x 1.125°
CMCC-CM2-SR5	1.25 x 0.9375°
KIOST-ESM	1.875 x 1.875
MIROC6	1.4° x 1.4°
NESM3	1.875 x 1.875
MRI-ESM2-0	1.125 x 1.125
CMCC-ESM2	1.4x1.4
HadGEM3-GC3-LL	1.875 x 1.25
ACCESS-CM2	1.9 x 1.3
IPSL-CM6A-LR	1.25 x 2.5
CNRM-CM6-1	1.4 x 1.4
MIROC-ES2H	1.4 x 1.4
MPI-ESM1-2-LR	1.875 x 1.875

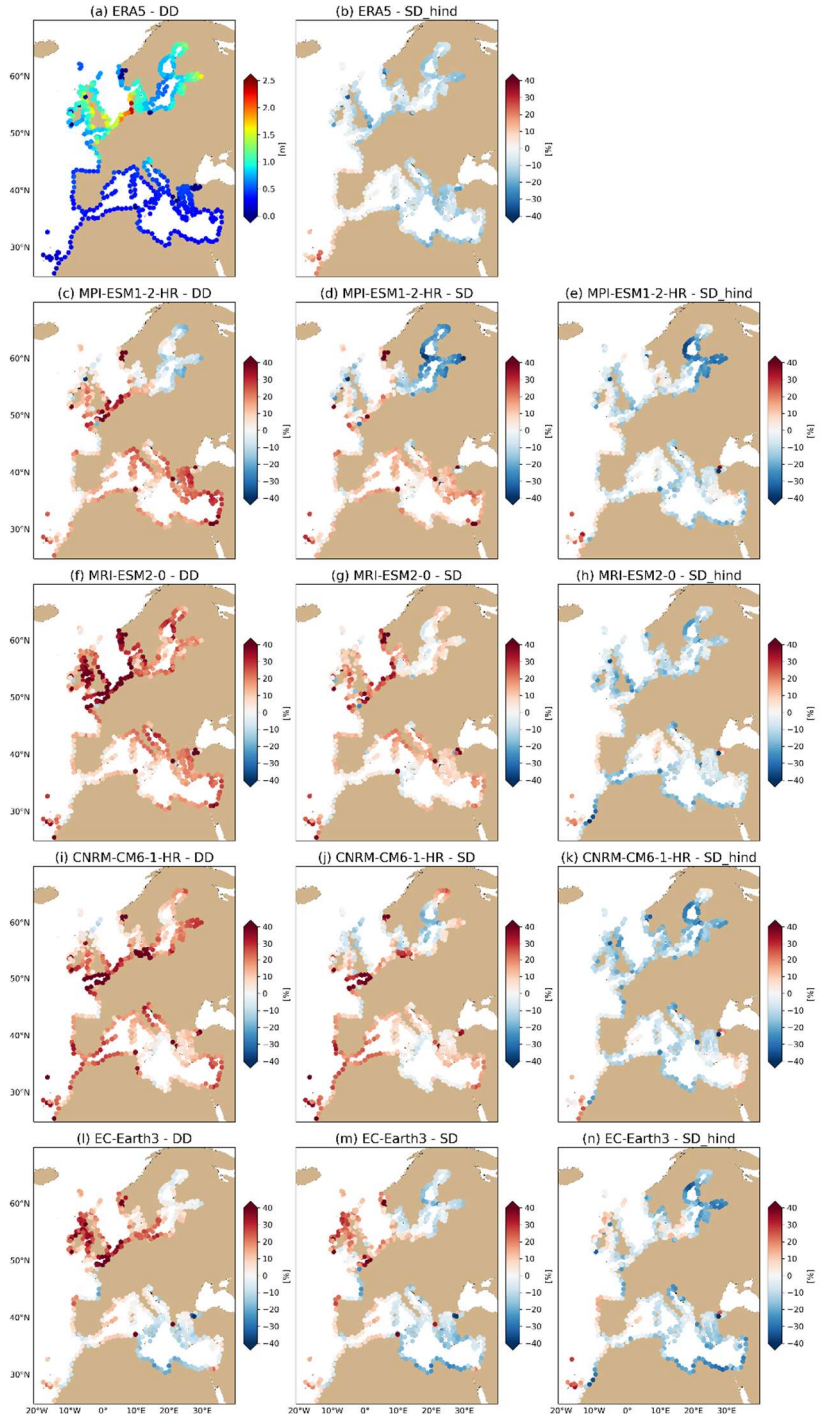

Figure S1 Validation against the hindcast dynamical simulation (panel a) of the 10-year storm surge return level from historical storm surge climate simulations: using the dynamical ensemble (c,f,i,l), using the statistical downscaling model (SDM) trained in the historical period for each GCM (d,g,k,m) and the SDM trained in the hindcast simulation (e,h,k,n). All pannels indicate relative differences [%] with the hindcast (panel a). Return levels are derived via stationary extreme value analysis on 1995-2014 for all

experiments except for the dynamically downscaled hindcast, for which a slightly different 20-yr period is used based on the simulation coverage (1997-2016). The SDM reconstruction of the hindcast simulation (b) is added for reference.

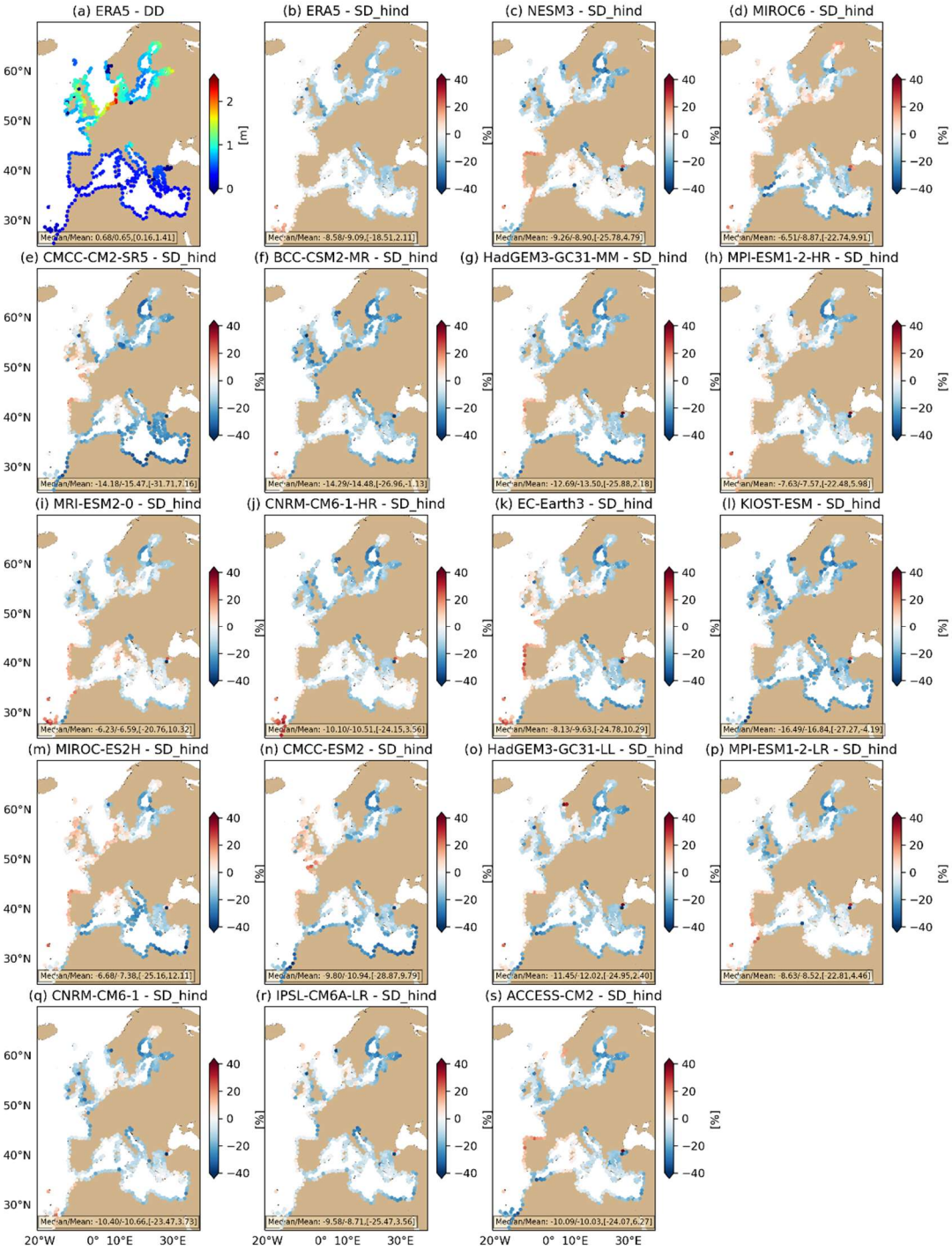

Figure S2 Validation against the hindcast dynamical simulation (a) of the 10-year storm surge return level (stationary EVA on 30 years, 1985-2014) from statistical storm surge estimates for historical climates given by each GCM in the 17-model ensemble. All pannels indicate relative differences [%] with to the hindcast (a). Median and mean values across coastal points are indicated, as well as the [5th, 95th] percentiles.

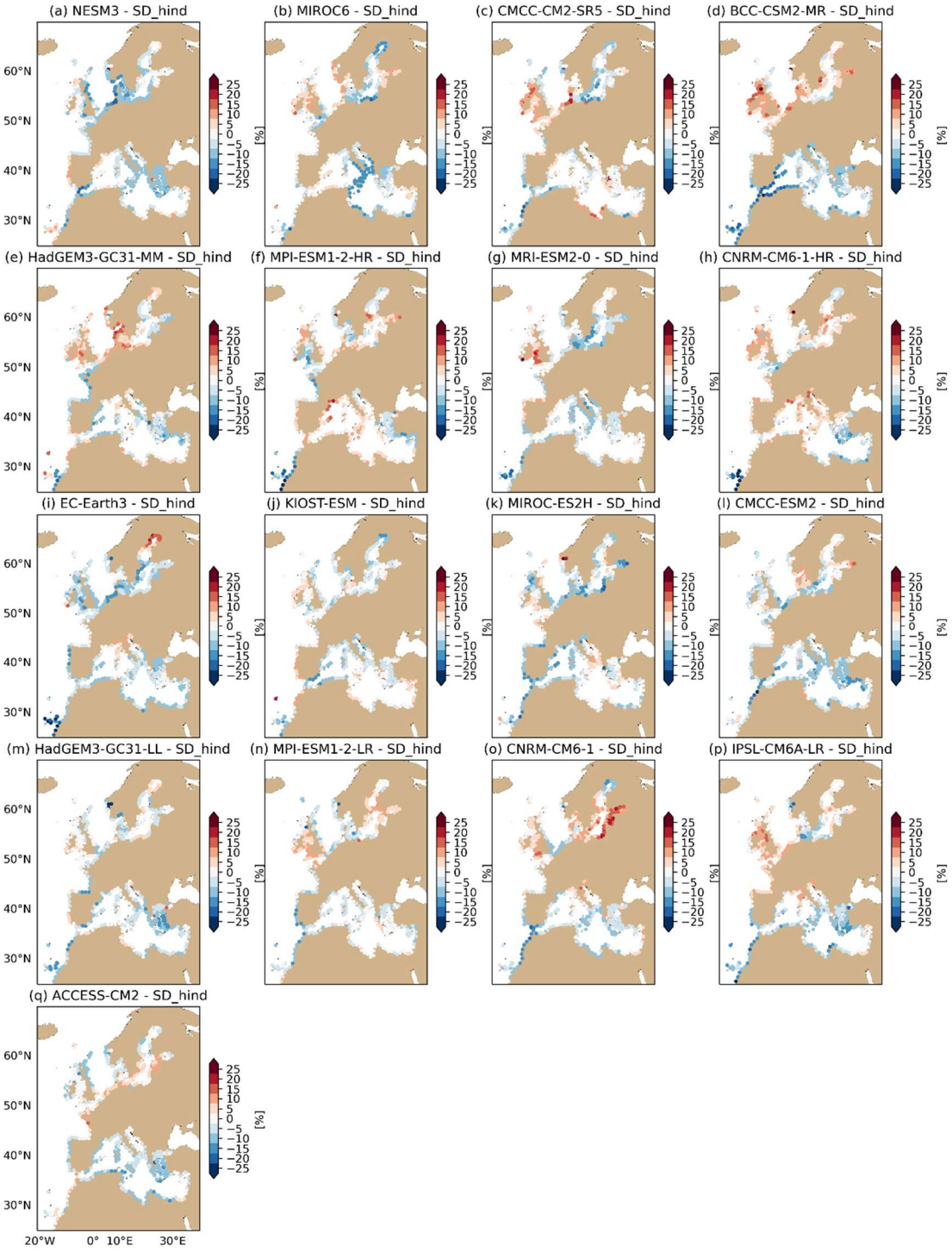

Figure S3 Projections of changes [%] in the storm surge 10-year return level (RL10) for the middle of the 21st century (stationary extreme value analysis on [2035-2064] vs [1985-2014]) for each of the 17 GCM models in the ensemble. Median and mean values across coastal points are indicated, as well as the [5th, 95th] percentiles.

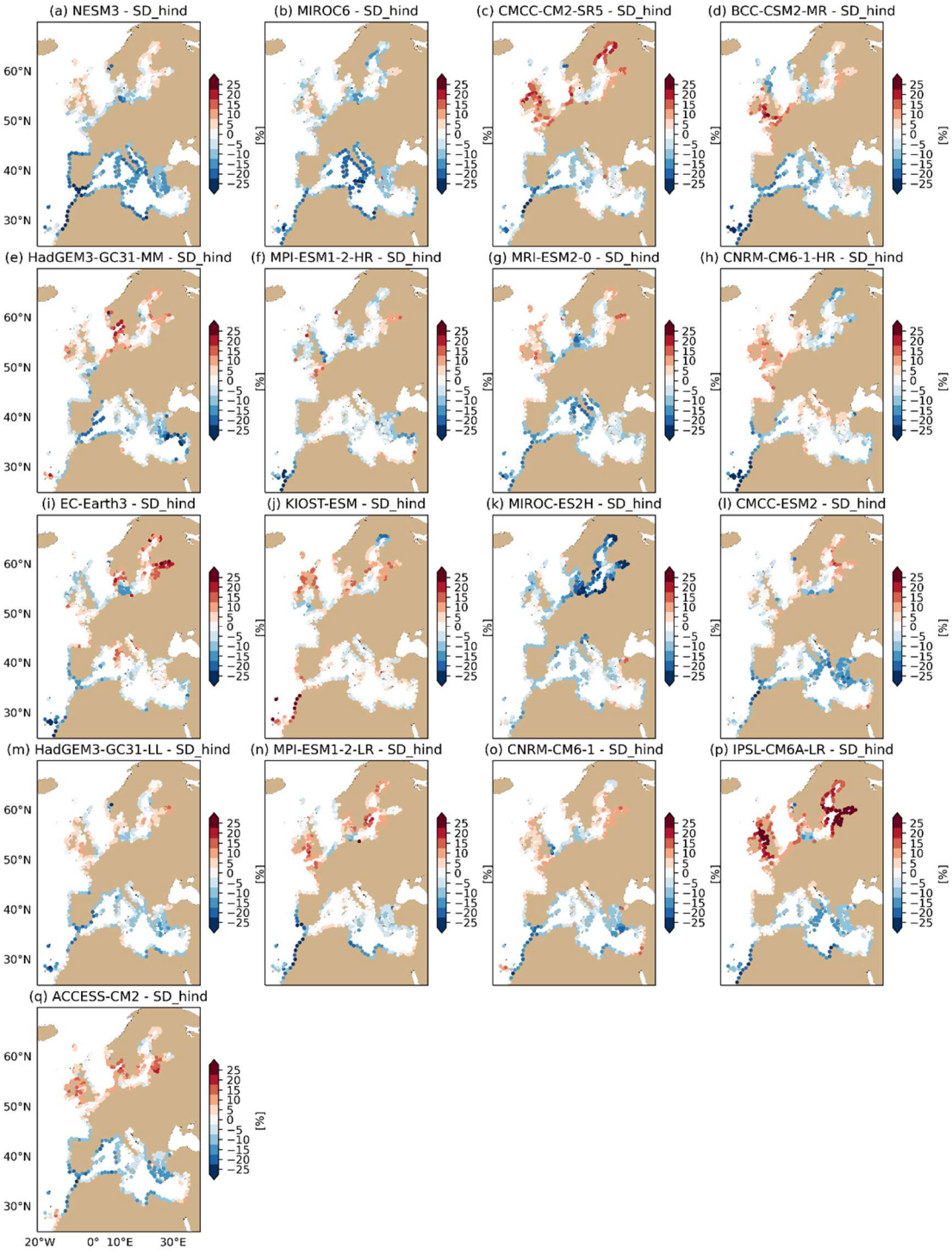

Figure S4 Projections of changes [%] in the storm surge 10-year return level (RL10) for the end of the 21st century (stationary extreme value analysis on [2070-2099] vs [1985-2014]) for each of the 17 GCM models in the ensemble. Median and mean values across coastal points are indicated, as well as the [5th, 95th] percentiles

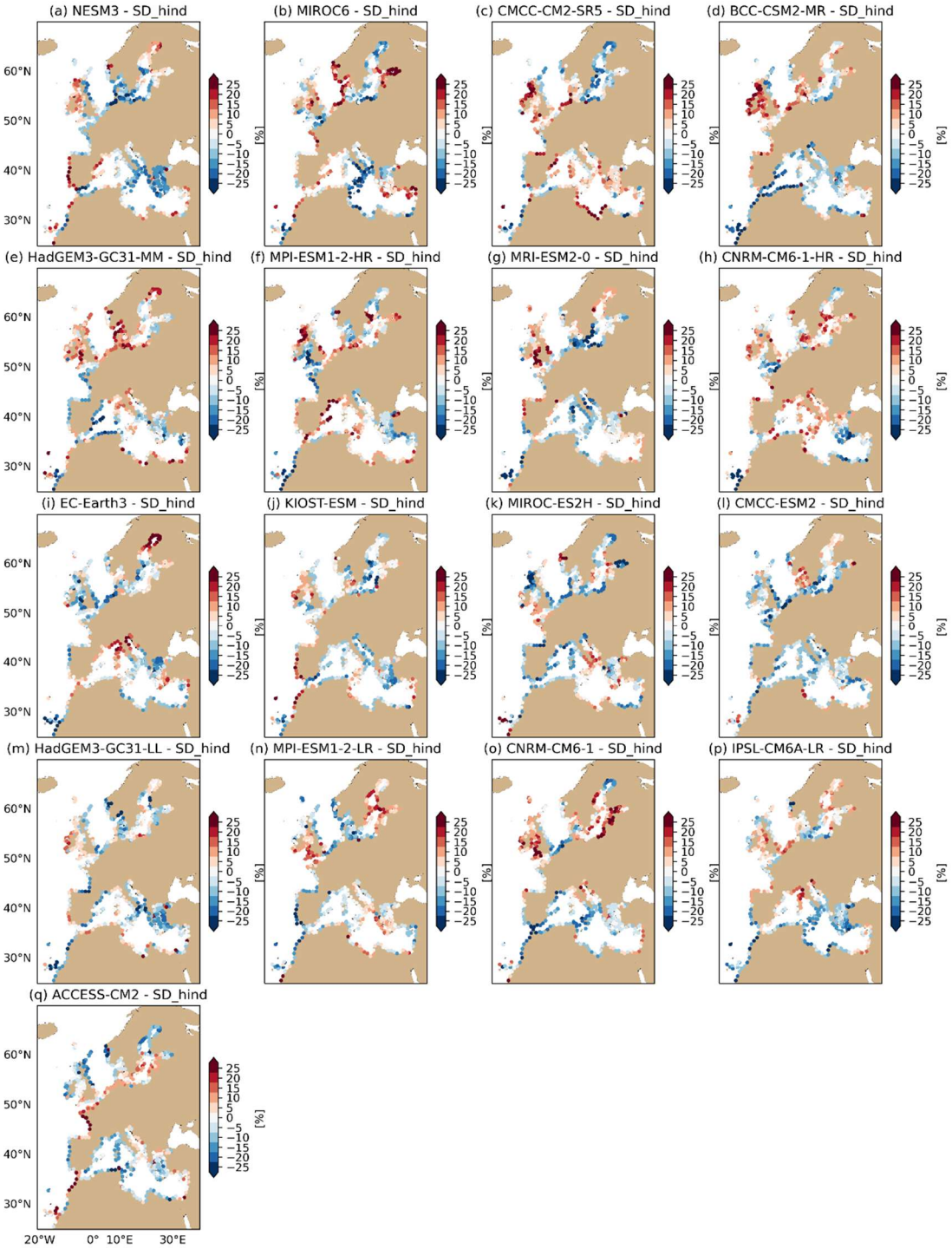

25 **Figure S5 Projections of changes [%] in the storm surge 100-year return level (RL100) for the middle of the 21st century (stationary extreme value analysis on [2035-2064] vs [1985-2014]) for each of the 17 GCM models in the ensemble. Median and mean values across coastal points are indicated, as well as the [5th, 95th] percentiles**

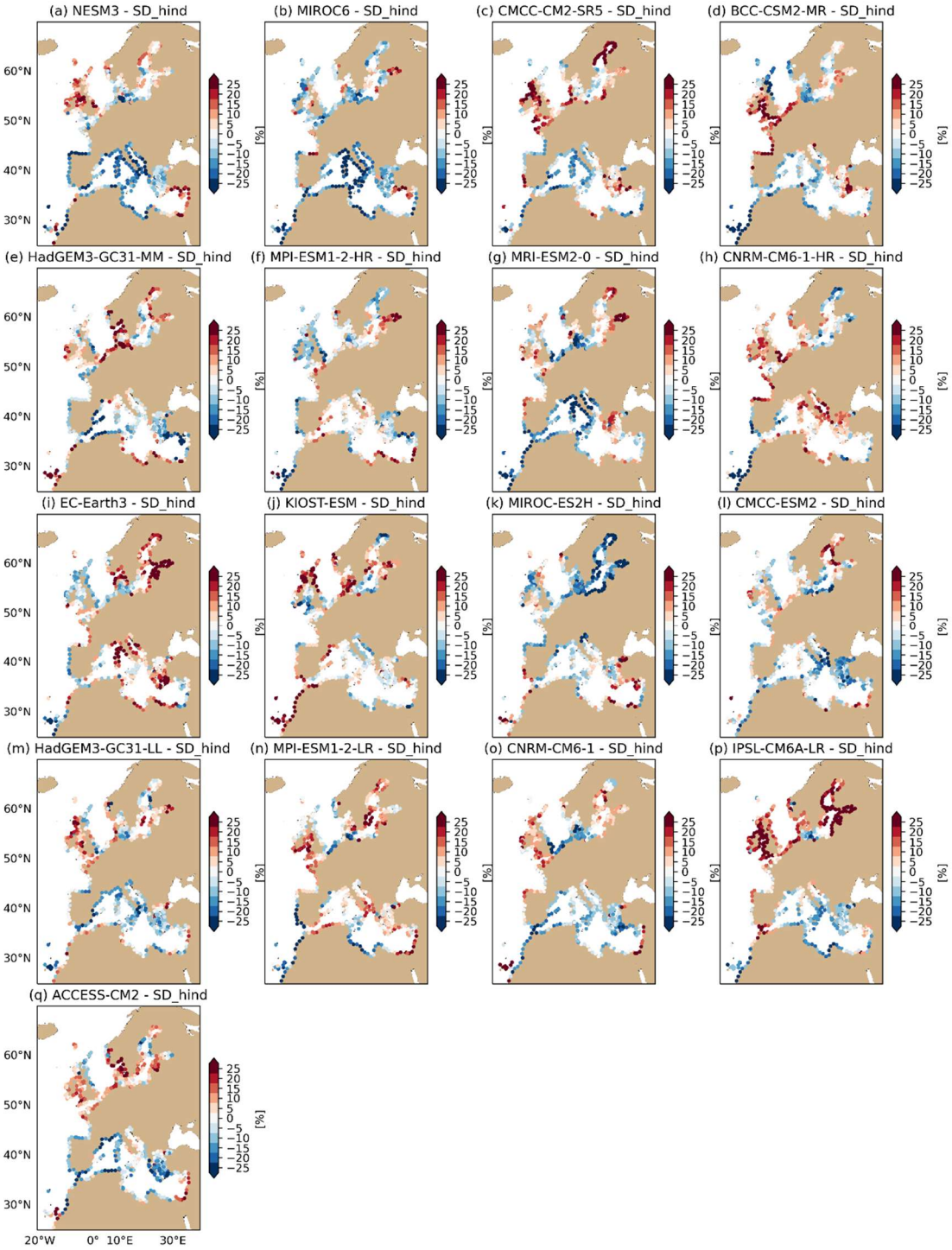

Figure S6 Projections of changes [%] in the storm surge 100-year return level (RL100) for the end of the 21st century (stationary extreme value analysis on [2070-2099] vs [1985-2014]) for each of the 17 GCM models in the ensemble. Median and mean values across coastal points are indicated, as well as the [5th, 95th] percentiles

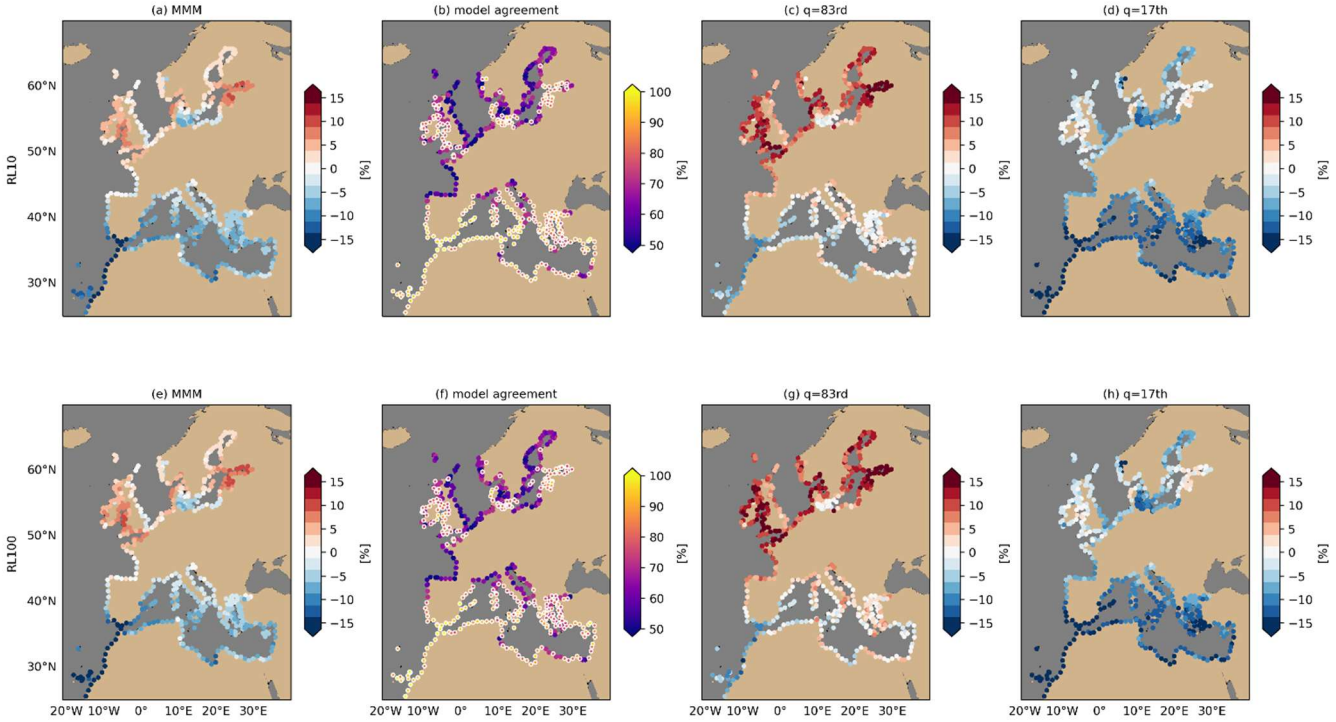

Figure S7 Projected RL10 (top) and RL100 (bottom) changes [%] by the end-of century when keeping the shape parameter in the GPD distribution constant in the future. Multi-model mean (MMM, first column), ratio of models agreeing in the sign of projected changes (second column), 83rd (third column) and17th (fourth columns) percentiles of projected changes in ensemble, indicating the likely range as per IPCC definitions. EVA is computed for 30 year periods: baseline [1895-2014] and end of the century [2070-2100]. For reference, in a 17-model ensemble, the 17th and 83rd quantiles correspond to the lower/higher ~3 models. The % model agreement represents the confidence on the sign of projected changes. Those with ratio >80% (here, >=13/17 models) are marked with romboids.

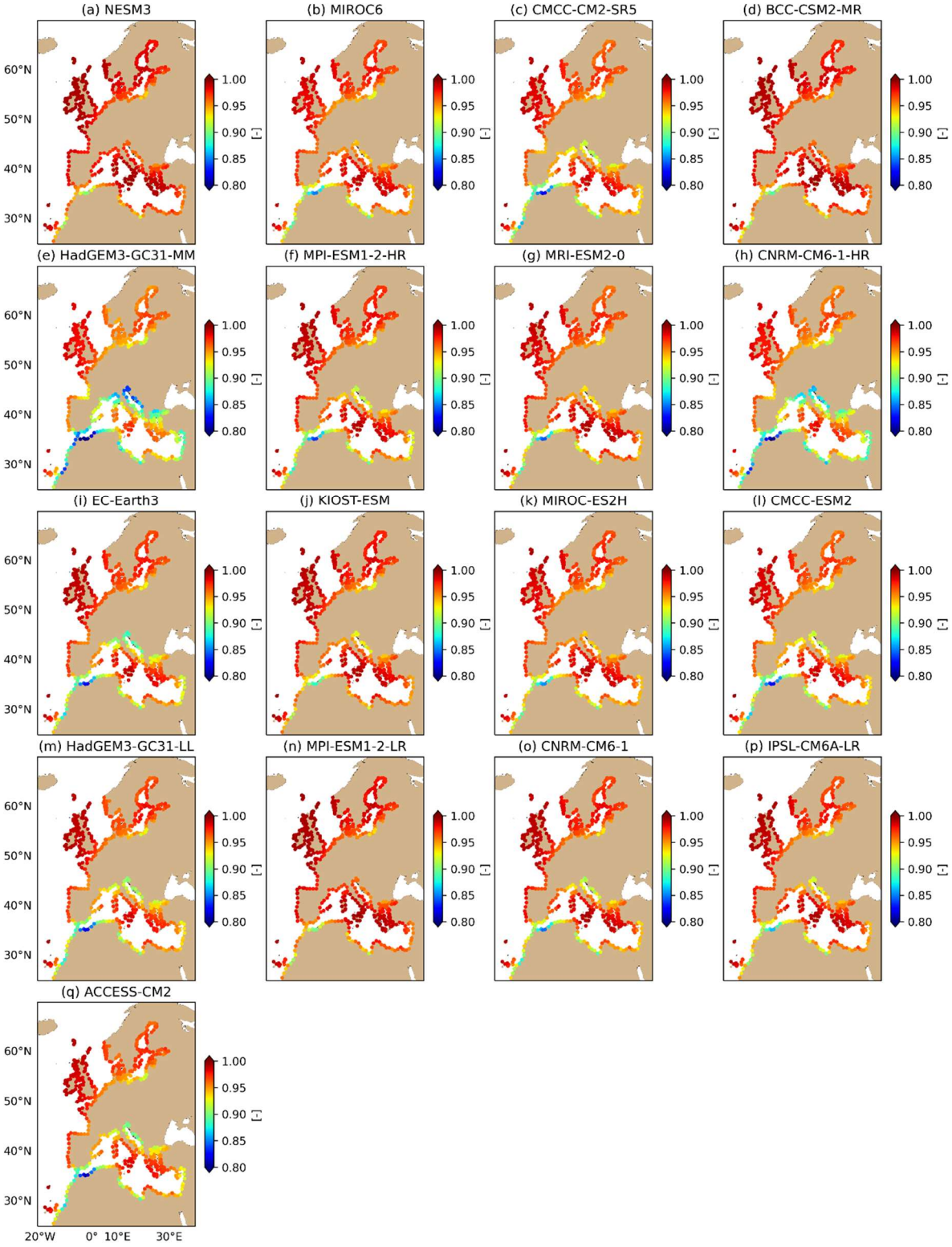
(a) NESM3
(b) MIROC6
(c) CMCC-CM2-SR5
(d) BCC-CSM2-MR
(e) HadGEM3-GC31-MM
(f) MPI-ESM1-2-HR
(g) MRI-ESM2-0
(h) CNRM-CM6-1-HR
(i) EC-Earth3
(j) KIOST-ESM
(k) MIROC-ES2H
(l) CMCC-ESM2
(m) HadGEM3-GC31-LL
(n) MPI-ESM1-2-LR
(o) CNRM-CM6-1
(p) IPSL-CM6A-LR
(q) ACCESS-CM2
60°N
50°N
40°N
30°N
20°W
0°
10°E
30°E
1.00
0.95
0.90
0.85
0.80
[-]

Figure S8 Explained total variance in the period 1995-2014 by the principal components resulting from the projection of the bias-corrected CMIP6 GCM atmospheric fields onto the empirical orthogonal functions (EOF) identified from training the statistical downscaling model on the hindcast simulation (*SD_hind*, i.e. EOFs extracted for the ERA5 reanalysis in 1997-2021).